ACS APPLIED MATERIALS & INTERFACES

Research Article

www.acsami.org

Hybrid PVDF/PVDF-*graft*-PEGMA Membranes for Improved Interface Strength and Lifetime of PEDOT:PSS/PVDF/Ionic Liquid Actuators

Aiva Simaite,*[,†,‡] Bertrand Tondu,[†,‡] Philippe Souères,[†,¶] and Christian Bergaud*[,†,¶]

[†]CNRS, Laboratoire d'Analyse et d'Architecture des Systèmes (LAAS), 7 avenue du Colonel Roche, F-31031, Toulouse, France

[‡]Université de Toulouse, Institut National des Sciences Appliquées (INSA), Laboratoire d'Analyse et d'Architecture des Systèmes (LAAS), F-31400, Toulouse, France

[¶]Université de Toulouse, Laboratoire d'Analyse et d'Architecture des Systèmes (LAAS), F-31400, Toulouse, France

Supporting Information

ABSTRACT: The exploitation of soft conducting polymer-based actuators suffers from two main shortcomings: their short life cycle and the reproducibility of the fabrication techniques. The short life cycle usually results from the delamination of the components due to stresses at the interface during the actuation. In this work, to achieve strong adhesion to poly(3,4- ethylenedioxythiophene) poly(styrenesulfonate) (PEDOT:PSS) electrodes, the wetting properties of the surface of a polyvinylidene fluoride (PVDF) membrane are improved using argon-plasma-induced surface polymerization of poly(ethylene glycol) monomethyl ether methacrylate (PEGMA). Hybrid membranes are created with hydrophilic PVDF-*graft*-PEGMA outer surfaces and hydrophobic bulk. The width of each layer is controlled by spray coating, as it allows for the deposition of the reaction precursor to a certain depth. Subsequently, a PEDOT:PSS water solution fills the pores of the functionalized part of the membrane and a mixing layer between PEDOT:PSS and PVDF is created. We also show that PVDF-*graft*-PEGMA copolymers play an important role in binding the membrane to the electrodes and that direct mechanical interlocking in the pores can further improve the adhesion. Finally, PEDOT:PSS/PVDF-*graft*-PEGMA/PEDOT:PSS actuators are made by simple solution casting. They are capable of producing high strains of 0.6% and show no signs of delamination after more than 150 h or 10^4 actuation cycles. Furthermore, the preservation of the hydrophobic membrane in between two PEDOT:PSS layers increases the resistance between them from 0.36 Ω to 0.16 MΩ, thus drastically modifying the power dissipation of the actuators.

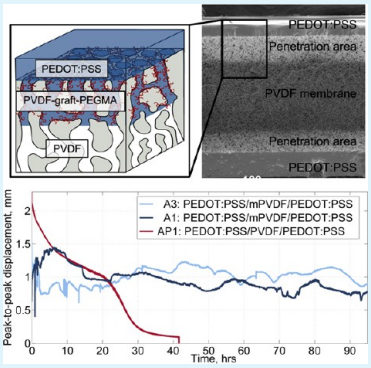

KEYWORDS: *surface adhesion, composite membrane, graft polymerization, interface, PEDOT, PSS, PVDF, ionic actuators, lifetime*

1. INTRODUCTION

Ionic electroactive polymer (iEAP)-based artificial muscles are a promising alternative to traditional actuators, especially when compliant skeletal musclelike response is desirable. Their work density and power-to-mass ratio are especially advantageous for creating agile microrobots; softness and biocompatibility may also favor their applications in medicine.[1−3] Prevalent iEAP actuators are composed of three layers: an ion storing membrane sandwiched between two electrodes. Small applied voltage (1−2 V) leads to the motion of ions and solvent in the membrane and the structure bends due to their consequent nonuniform distribution. The use of conducting polymers (CPAs) instead of metal electrodes decreased the rigidity and brittleness of the trilayer and improved their lifetime.[4] In addition, in CPAs, oxidation or reduction of the polymer is followed by the electrochemical ion insertion and removal between the polymer chains. This causes its volume change and is considered to be the primary factor leading to the actuation.

Two processes limit the lifetime of the conducting polymer actuators: (1) degradation of the polymer or decomposition of the electrolyte under electrochemical cycling and (2) delamination of the electrodes from the membrane due to stresses at the interface.[5,6] Higher electrochemical window of ionic liquids reduces the degradation effect.[7,8] Furthermore, their nonvolatility enables longer actuation in air.[9,10] Nevertheless, the delamination of layers constituting an actuator is still a common problem. When conducting polymers are synthesized directly on the membrane, the produced interfacial layer prevails for thousands of cycles but adverse partial connections between electrodes are often created.[11−13] When the actuators are electropolymerized on gold as a substrate, surface roughening methods are required to prevent fast delamination.[6]

The availability of water-soluble poly(3,4-ethylene dioxythiophene) polystyrenesulfonate (PEDOT:PSS) conducting polymer has led to several attempts to fabricate actuators via solution casting.[10,14−16] Yet, PEDOT:PSS aqueous solutions have a high surface tension of 70.2 mN/m, causing poor

Received: May 26, 2015
Accepted: August 20, 2015
Published: August 20, 2015

DOI: 10.1021/acsami.5b04578
ACS Appl. Mater. Interfaces 2015, 7, 19966−19977

Scheme 1. SEM Photomicrograph of the Cross-Section of PEDOT:PSS/PVDF-Graft-PEG/PEDOT:PSS Trilayer Actuator with the Depth of Penetration Visible as Brighter Areas on the Membrane ((Left) Scheme of PVDF, PVDF-Graft-PEGMA, and PEDOT:PSS Interfaces and (Right) AFM Surface Scan Images of PVDF Membrane before Functionalization)

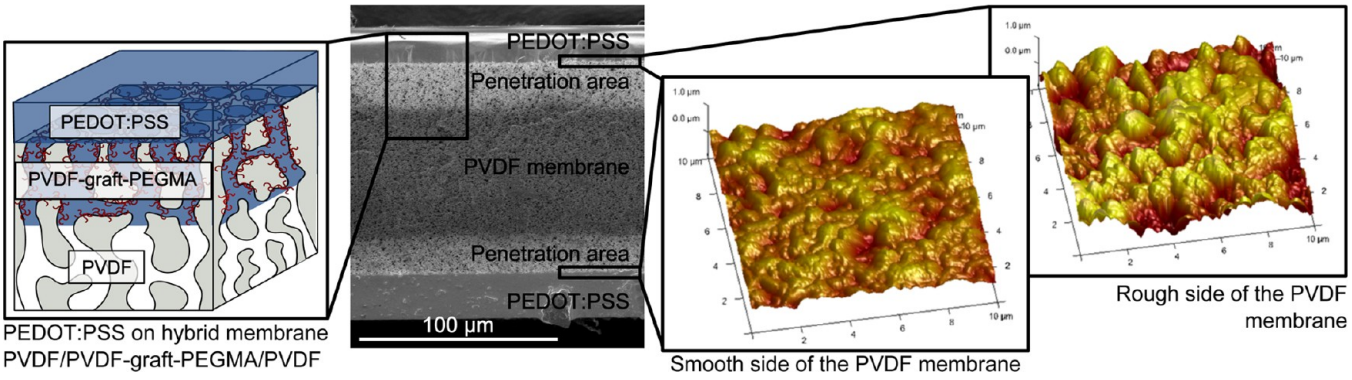

wetting and weak adhesion to many substrates.[17,18] Because of its remarkable chemical and temperature stability, as well as good ionic conductivity and excellent mechanical properties (low Young's modulus, high breaking stress, etc.), poly(vinylidene fluoride) (PVDF) is preferred as an ion storing membrane.[19] Unfortunately, it is also one of the polymers with the lowest surface energy (25 mN/m) and is highly hydrophobic (water contact angle of >130°).[20,21] Not surprisingly, the interface of PEDOT:PSS film and the PVDF membrane does not outlast immersion in ionic liquid.[16] The use of other than PVDF membranes is considered as an alternative but at a cost of significantly lower ionic conductivity (19.4 mS/cm vs 0.9 mS/cm) for PVDF and polyurethane in emimTFSI.[10,12] PEDOT:PSS is promising because of its electrical conductivity, which reaches 3000 S/cm.[22] Therefore, a method to improve their adhesion is needed.

Good adhesion between two polymers requires certain depth of entanglement of their chains. Compatibility of the chemical nature of materials is essential and interfaces are generally weak, unless chemical bonding (hydrogen, covalent etc.) stabilizes them.[23,24] Therefore, the addition of hydrophilic moieties on the surface, damage by plasma, and grafting of more-flexible chains are often used as adhesion enhancers.[25−28] Surfaces functionalized with grafted hydrophilic polymer chains were reported to improve adhesion strength between two grafted surfaces and to materials deposited on them.[29,30] This strategy was also used by Ikushima et al. to improve adhesion between PVDF and PEDOT:PSS but was not discussed in detail.[16] In this report, we (1) suggest an argon-plasma-induced "grafting-to" method that allows partial hydrophilization of the PVDF membrane, (2) discuss factors playing an important role in adhesion between the membrane and the solvent-casted polymer film, and (3) report the influence of the mixing depth on the lifetime and performance of the trilayer conducting polymer-based actuators.

Surface modification of PVDF membrane by argon-plasma-induced graft polymerization of hydrophilic poly(ethylene glycol) (PEG) or its monomethyl ether methacrylate (PEGMA) is often used in order to improve membrane antifouling properties.[31−34] Plasma activates the PVDF surface, creating chain scissions and relatively stable radicals. These radicals can then participate in chemical reaction. Nevertheless, post-irradiation reactions are difficult to control and a relatively high amount of material is cross-polymerizing, possibly blocking the pores of the membrane and further increasing its asymmetry.[35−38] Alternatively, a reaction precursor can be deposited on the membrane *a priori* and grafted during the irradiation.[31,33,34] This generally leads to a thinner grafted layer and grafting weight can be controlled by irradiation time, plasma power, and amount of the precursor. As radicals are generated on both the substrate and the precursor, they lead to the competing reactions of (1) the substrate and the polymer, (2) cross-linking of polymers, and (3) cross-linking of the substrate.[34] The resulting structure of the graft polymer is more difficult to predict and is less defined, and brushlike, network-like, etc. morphologies can be obtained, depending on the plasma conditions.[33] Besides, etching and degradation effects will play a role after longer grafting times, competing with polymerization.[34,39]

Reaction during irradiation leads to the very thin grafting layer, on the order of 7.5 nm, that does not change the porosity and does not affect mechanical and thermal properties of the membranes.[31,34] However, in most of the previously reported cases, pores of the membrane were activated, leading to grafting through the membranes.[31,33−35,37,38] The main parameters influencing plasma penetration depth are membrane porosity, plasma power, and pressure. However, even for a pore size of 0.1 μm and at atmospheric pressure, membrane activation inside the pores can occur.[33,38] This was confirmed by our preliminary experiments. PEGMA adsorbs on the pore walls of the PVDF when membrane is incubated in its solution and subsequent grafting during irradiation leads to functionalization of the membrane to at least half of its thickness. Consequent grafting on the opposite side of the same membrane causes full hydrophilization; that is not desirable for our application.

In the first part of the article, we suggest a fabrication technique that allows partial functionalization of PVDF membranes. Instead of controlling plasma penetration depth, we deposit reaction precursor on only the outer surfaces of PVDF membrane by spray-coating. In this case, PVDF is activated all the way through its thickness, but it is hydrophilized only to a certain depth. Subsequently, the infiltration depth of PEDOT:PSS aqueous solution into the pores of the membrane will be determined by the depth of the created hydrophilic layer, as shown in Scheme 1. The hydrophilization depth can be tuned by changing spray coating parameters and hybrid hydrophilic−hydrophobic−hydrophilic membranes can be fabricated (see the SEM photomicrograph in Scheme 1).

DOI: 10.1021/acsami.5b04578
ACS Appl. Mater. Interfaces 2015, 7, 19966−19977

Scheme 2. Fabrication Steps and Processes Towards Functionalization of PVDF Membranes: (Left) Reaction Precursor (PEGMA Macromonomer) Deposited on the Upper Surface of the PVDF Membrane by Spray Coating; (Middle) PVDF Membrane with Dried PEGMA Treated with Low-Pressure Argon Plasma;[a] (Right) Hybrid PVDF/PVDF-*graft*-PEGMA Membranes Produced after Residual PEGMA Precursor Has Been Washed Away

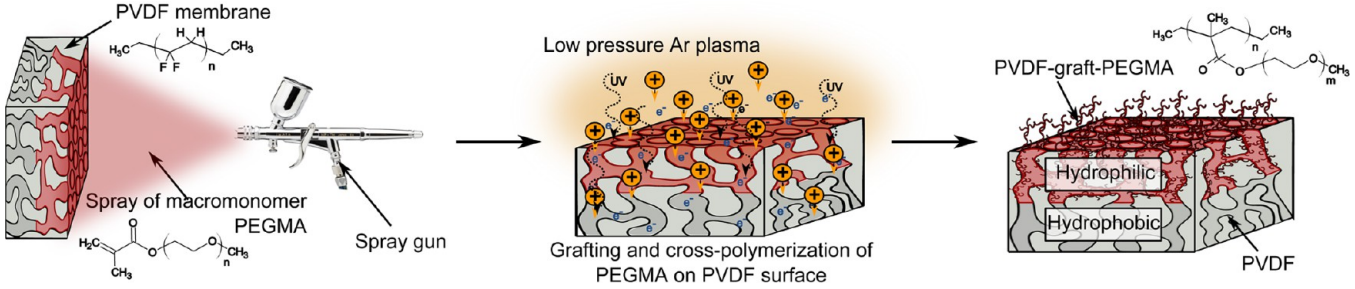

[a]Plasma penetrates through into the pores of the membrane, creating radicals on PVDF and initiating the "grafting-to" reaction and PEGMA polymerization.

Commercial PVDF membranes are slightly asymmetrical (AFM surfaces scans are shown in Scheme 1), and their surface roughness has important consequences on the PEGMA deposition process, grafting during irradiation and, finally, adhesion to PEDOT:PSS. In the second part of the article, we demonstrate the importance of the grafted surface on adhesion. We also comment on other important aspects that must be taken into account when designing strong interfaces, such as the influence of surfactants and hydrophilic coating of the membrane.

Finally, we also report the simple and successful fabrication of PEDOT:PSS/PVDF/PEDOT:PSS-based actuators by drop-casting. We show that trilayers with good adhesion between different layers can be actuated for more than 10^4 cycles at 0.1 Hz and more than 150 h in air without any signs of delamination. Furthermore, the interface is also strong enough to sustain strains of more than 0.6%. This is an important step toward long lifetime and stable actuators.

2. RESULTS AND DISCUSSION

2.1. Functionalization of PVDF Membranes: Surface. For prevalent membrane functionalization during plasma irradiation, the reaction precursor is usually deposited by incubating the membrane in the precursor's solution. In the case of PEG or PEGMA, it leads to their adsorption on all the surface of the membrane, including the surface of the pores. Subsequently, exposure to low-pressure argon plasma hydrophilizes the membrane through its thickness as was confirmed by our preliminary experiments. Two adjustments to the process were considered in order to limit the grafting: (1) limiting the depth of the activation by plasma and (2) limiting the availability of precursor to a certain thickness (summarized in Scheme S1 in the Supporting Information). Controlling low-pressure gas diffusion in the membrane is a challenging task, thus blocking the pores of the membrane is one way to restrict it path to the surface. This can be achieved by impregnating the membrane with highly viscous fluid, such as PEG or PEGMA. Even though this is a valid method (Figures S2 and S3 in the Supporting Information), the functionalization is limited to only the outer surface (few micrometers). On the other hand, the method to limit the availability of the reaction precursor gives a way to control the width of the hydrophilic layer.

PEGMA is an amphiphile that immediately adsorbs on the walls of a hydrophobic PVDF membrane. Therefore, very small quantities of PEGMA must be deposited in order to prevent its infiltration in the pores. This can be achieved by air spray coating (Scheme 2). The spray is produced when the compressed air stream is mixed with the solution. An optimized spray process leads to a deposition of the small quantities of the materials in an almost solvent-free state. Therefore, we assume that, when PEGMA droplets reach the PVDF surface, its spreading and infiltration will be mainly driven by its surface diffusion.[40] Theoretical studies of the nature of the polymer adsorption and the surface kinetics are still a large challenge in the field.[41] Nevertheless, its surface diffusion rate in a concentrated layer (e.g., after solvent evaporation) is 10 times slower than in solution, and it is likely that the residual solvent is an essential condition for lateral diffusion into the pores.[42,43]

The droplet size just before the impact and, consequently, the amount of the residual solvent are dependent on many conditions, e.g., ejection speed, initial droplet size, time-of-flight, solvent evaporation rate (some spraying parameters that can influence them are shown in Figure S4 in the Supporting Information). In our case, 10 vol % PEGMA solution in a 10 vol % ethanol/water azeotropic mixture was used, since it was shown to lead to the most homogeneous deposition. The amount of PEGMA sprayed (spray density (SD) is defined as the deposited weight per flat outer surface area) was varied by controlling the distance of the spray coater (from 25 cm to 35 cm) and the sprayed solution volume (from 0.5 mL to 2.0 mL). Dried membranes with deposited PEGMA were then irradiated by low-pressure argon plasma, as depicted in Scheme 2.

As shown in Figure 1, the PEG density grafted on the PVDF surface (GD, defined as the weight increase per flat outer surface area) is dependent on the spray coating (SD). GD increases almost linearly with the density of the sprayed precursor, for SD < 1 ng/mm^2; however, SD > 2 ng/mm^2 leads to less grafting. Etching during plasma treatment could be one of the explanations; nevertheless, it is unlikely during short (15 s) irradiation.[34] The decline in the grafting yield could also be explained by fast PEGMA cross-polymerization on the outer surface and dense coverage, preventing activation of the PVDF pores. This possibility is supported by AFM surface scans and attenuated total reflectance-Fourier transform infrared (ATR–FTIR) measurements (Figure S5 in the Supporting Information) of membranes prepared using different irradiation times (preliminary experiments). The surface coverage is the smoothest after only 20 s of irradiation, and a significant increase in roughness (from 188 nm to 435 nm) is observed for longer grafting. Moreover, ATR–FTIR measurements show an

DOI: 10.1021/acsami.5b04578
ACS Appl. Mater. Interfaces 2015, 7, 19966–19977

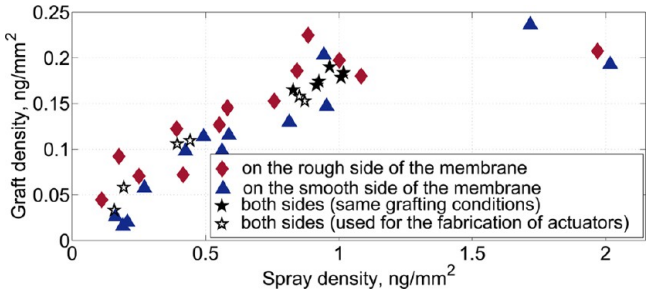

Figure 1. Grafting density (GD) versus density of PEGMA sprayed (SD) on the rough (red diamonds, ♦) and smooth (blue triangles, ▲) sides of the membrane under different grafting conditions. Solid black stars (★) show results obtained at the same grafting conditions, i.e., reproducibility of the process. Open stars (☆) correspond to the SD and GD values of the membranes used to fabricate the actuators.

increase in OCO/CF ratio of the membrane, indicating dense coverage. For 30 s of grafting on the rough side of the membrane, the CF signal is almost gone, most likely due to roughness, which prevents IR wavelength from reaching the membrane. These results corroborate with the idea of the faster reaction on the uppermost areas of the membrane. For further experiments, a shorter irradiation time of 15 s was used.

By changing the distance of the spray gun to the membrane from 35 cm to 20 cm (i.e., the size of the droplet that reaches the membrane is changed), a large spectrum of SD and GD values was obtained, as shown in Figures 2a and 2b. Even small amounts of PEGMA sprayed (SD and GD values are indicated in the legend) lead to reaction on the surface and its full coverage, as suggested by saturation of the OCO/CF ratio of

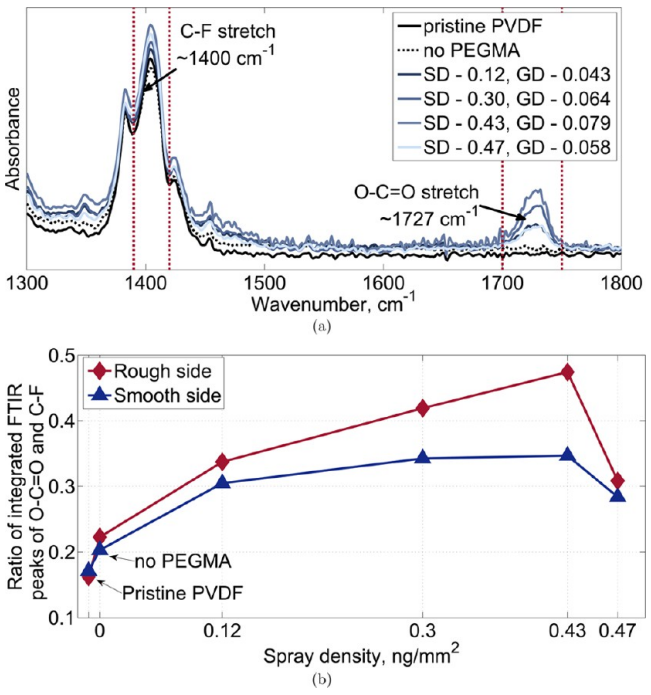

Figure 2. (a) FTIR absorption spectra of PVDF membranes with different spray (SD) and grafting (GD) densities. The wavelengths corresponding to CF and OCO vibrations are indicated with arrows. Red dotted line marks the integration region used to calculate the peak ratio. (b) Ratio of integrated OCO and CF peaks of pristine (indicated with an arrow) and functionalized PVDF membranes versus sprayed amount of precursor (PEGMA).

the membranes grafted on the smooth side. As the roughness of the surface further increases for the grafting on the rough side (Figure 4 and Figure S6 in the Supporting Information), larger OCO/CF ratio could be explained as a result of decreased accessibility of the membrane to IR wavelength. Interestingly, large amounts of PEGMA deposited (SD = 0.47 ng/mm^2) lead to relatively low grafting densities (GD = 0.058 ng/mm^2). That is also an indication of the fast and dense surface coverage, which might prevent plasma from reaching precursor in the pores.

Figure 3 shows the dependence of the water contact angle (WCA) on surface roughness and chemical composition. For

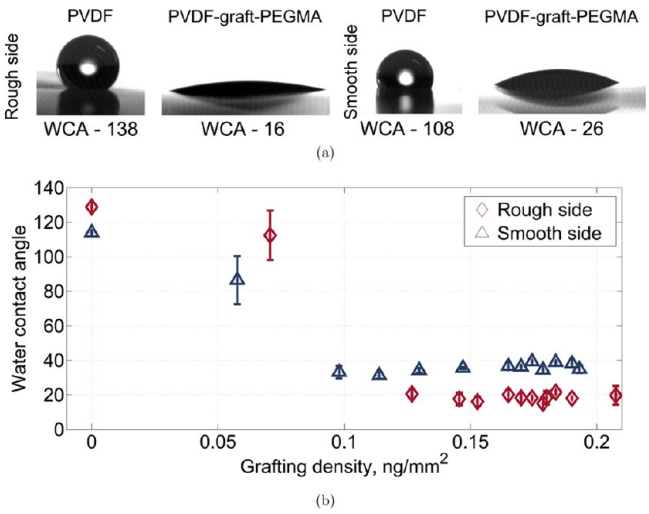

Figure 3. (a) Pictures of water drops on functionalized and pristine PVDF membranes and (b) water contact angle (WCA) of pristine PVDF and PVDF-*graft*-PEGMA membranes at different grafting densities.

pristine membranes, WCA = 130° and 110° for the smooth and rough side, respectively. Surface roughness influences wetting, in the sense that the WCA on the rough chemically hydrophobic surfaces is larger and WCA on the rough hydrophilic surfaces is even lower.[44] Therefore, WCA decreases much faster, to ~20°, when the rough side is functionalized. Grafting on the smooth side leads to a decrease to ~40°. It is also worth noting that even though small grafting densities (>0.06 ng/mm^2, which corresponds to an SD value of ~0.12 ng/mm^2 and OCO/CF ratio before saturation) lead to WCA lower than 100°, surface coverage is less homogeneous as suggested by high WCA measurement error. Therefore, for fabrication of the membranes, we suggest using a GD value of at least 0.07 ng/mm^2.

In summary, surface roughness of the substrate seems to influence PEGMA grafting behavior. When grafting on the rough side, slightly larger grafting efficiency can be expected as shown in Figure 1. Our results suggest that reaction might be faster on the uppermost areas of the membrane, further increasing its roughness (Figure 4 and Figure S6 in the Supporting Information). Surface coverage seems to be more homogeneous (no significant roughness change) on the smooth side. Finally, the surface area of the membrane (as measured by krypton adsorption and Brunauer–Emmett–Teller (BET) theory) does not change significantly with functionalization (5.19 ± 0.33 m^2/g for pristine and functionalized membranes), suggesting that, with the exception of the

DOI: 10.1021/acsami.5b04578
ACS Appl. Mater. Interfaces 2015, 7, 19966–19977

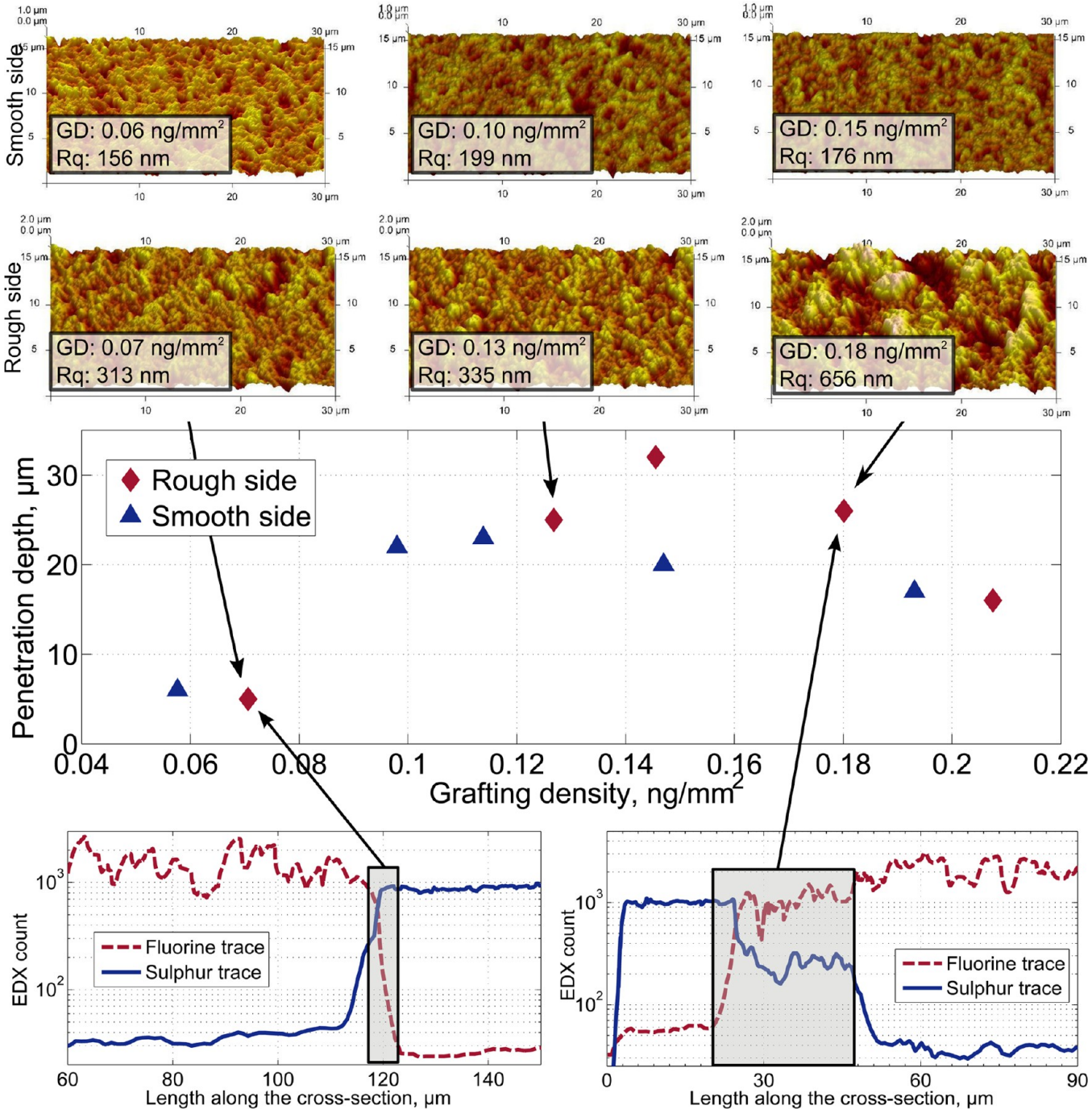

Figure 4. (Bottom) EDX line scans for sulfur (solid blue line) and fluorine (dashed red line) along the cross sections of PEDOT:PSS/PVDF-*graft*-PEG with the GD indicated with the arrows. (Center) The length of the depth of mixing versus the grafting density (GD) plotted separately for PEDOT:PSS deposited on the rough side (blue triangles, ▲) and the smooth side (red diamonds, ♦) of PVDF-*graft*-PEG. (Top) AFM images of the rough and smooth surfaces of the PVDF-*graft*-PEG membranes with different grafting densities (GD). GD and the roughness are indicated in the legends.

upper surface of the membrane, reaction is mostly restricted to a very thin layer.

2.2. Functionalization of PVDF Membranes: Pores of the Membrane. PEG and PEGMA are good wetting agents and are immediately adsorbed on the PVDF membrane. Compared to water, their aqueous solutions spread easier (WCA = 53.3° ± 2.3° and 39.3° ± 2.8° for 10 vol % solution on the rough and smooth sides of the pristine PVDF (pPVDF), respectively) and infiltrate into the PVDF pores. Therefore, during spraying, if PEGMA reaches the surface with a small amount of residual solvent, it is likely to diffuse to a certain depth. Since Ar plasma fills the pores of the membrane and is even further accelerated by biasing, the depth of the plasma-induced graft polymerization will be influenced by spraying parameters.

In order to estimate the grafting depth, elemental analysis by energy-dispersive X-ray (EDX) spectroscopy along the cross-section of the membrane was utilized. Since very small amounts

DOI: 10.1021/acsami.5b04578
ACS Appl. Mater. Interfaces 2015, 7, 19966−19977

of PEGMA are grafted (~1 mg per one side of the membrane), the thickness of the graft layers is probably smaller than 7.5 nm and PEGMA (oxygen trace) is not detectable by EDX analysis.[34] Therefore, we use a PVDF-*graft*-PEGMA/PEDOT:PSS sandwich for the indirect measurement of its depth of mixing. It was observed that PEDOT:PSS does not infiltrate into the pores of the pristine hydrophobic PVDF membrane (its EDX scan along the cross-section is shown in Figure S7a in the Supporting Information). Therefore, appearance of the depth of mixing is an indicator of the hydrophilization (Scheme 1). Traces of sulfur (the signature element of PEDOT:PSS) and fluorine (the signature element of the PVDF membrane) are shown in the bottom of Figure 4. The estimated depth of mixing is framed in black; it corresponds to the depth of plasma induced graft polymerization.

The thickness of the grafting depth increases with GD, up to ~30 μm, as shown in Figure 4. However, at higher grafting densities (>0.16 ng/mm^2), it seems to reach the saturation level and, after 0.18 ng/mm^2, even starts to decrease. This corroborates with our earlier assumption that, because of a fast PEGMA polymerization on the outer surface of the membrane, plasma diffusion deeper into PVDF pores is restricted. Furthermore, small differences might be observed for the mixing depth on the rough and smooth sides of the membrane: on the smooth side, it saturates at a lower depth. This again agrees with our assumption of the influence of the coverage on plasma diffusion, i.e., a smoother surface means a smaller surface area and higher actual grafting density for the same amount of PEGMA. Subsequently, this could lead to a faster reduction of pore size.

Based on these results, we suggest that two mechanisms compete during argon-plasma-induced graft polymerization: (1) plasma diffusion in PVDF, which results in a large grafting depth and thin PVDF-*graft*-PEGMA layers along the pores, and (2) cross-polymerization of PEGMA on the upper surface, which may cause a dense coverage and limit the plasma diffusion to smaller depths.

2.3. Strength of PEDOT:PSS/PVDF Interface. The first step toward the adhesion between materials is their intimate contact (i.e., good wetting). Subsequently, interdiffusion of polymers and their chain entanglement remove the boundary and create a strong interface.[45,46] The miscibility and mobility of polymers determine the diffusion rate and surface modification strategies are often used to improve it.[25,27,28] After PVDF modification with PEGMA, its contact angle with PEDOT:PSS water solution decreases from 132° and 116° (on the rough and smooth sides, respectively) to ~23° and ~28°, respectively. Functionalization provides chemical compatibility of materials and also creates a polymer layer that is hydrated and mobile in aqueous solutions.[29,33,47] Therefore, when PEDOT:PSS solution is put in contact with the PVDF-*graft*-PEGMA (mPVDF) surface, PEDOT:PSS adsorption out of the solution will take place. Contrary to pristine pPVDF, the grafted layer is expected to make the polymer interaction by hydrogen bonding possible, which subsequently could lead to entanglement of the polymers.

In order to estimate the adhesion strength between pPVDF and mPVDF membranes and solution-casted PEDOT:PSS films, the adhesive tape peel test was used (similar to ISO 2409:2013 recommendations and validated by Liu et al.[6] and Kim et al.[48]). Two series of parallel cuts cross-angled to each other to obtain a pattern of 25 similar squares was cut on the surface of PEDOT:PSS without slitting the membrane (steps shown in Figure 8). Then, the adhesive tape was applied and slowly removed. The procedure was repeated five times (Test I). Depending on the interface strength, the PEDOT:PSS film remained on the PVDF membrane or was removed with the adhesive tape. We would like to emphasize that these are qualitative "pass−fail" tests and do not provide any information on the value of the interface strength. Most of the following results provided in this section are observations; quantitative experiments are needed to verify them.

Results of the adhesion tests on pPVDF and mPVDF are shown in Figure 5. Higher surface roughness seems to have a positive influence on the adhesion strength of PEDOT:PSS to the membrane. Significantly larger area of PEDOT:PSS film remains on the rough side of PVDF after Test I. The influence of the surface roughness on adhesion is debatable; however, in this case, it is most likely due to the physical anchoring on the more frequent deep corrugations on the surface.[23,49] Nevertheless, adhesion is not strong enough to support stress induced at the interface once the membrane is placed into the ionic liquid (Test II). PEDOT:PSS that remained on the pPVDF after Test I was completely removed from it with five or less applications of adhesive tape in a soaked state.

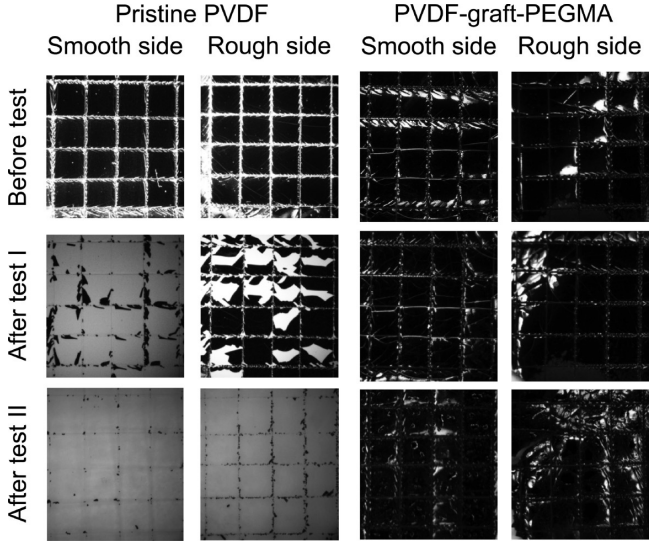

Figure 5. Qualitative adhesion test of PVDF and PVDF-*graft*-PEGMA membranes (white) and PEDOT:PSS (black). Pictures are taken after the grid was cut (before the test), after five adhesive tape peeling tests (Test I) and again after incubation of the bilayer in the ionic liquid for 24 h and five more peeling tests (Test II).

On the other hand, even a low density (GD = 0.07 ng/mm^2) of PVDF-*graft*-PEGMA leads to significantly improved adhesion strength. PEDOT:PSS film remains on the mPVDF membrane surface after tests in a dry state and after immersion in ionic liquid (Figure 5). Three mechanisms could explain stronger interface: (1) hydrogen bonding between PEGMA and PEDOT or PSS polymers; (2) entanglement of PEDOT and PSS with the graft-PEGMA layer; and (3) infiltration and mechanical interlocking of the PEDOT:PSS film in the pores of membrane.

A GD value of ~0.07 ng/mm^2 creates an interfacial layer of only few micrometers, as was shown in Figure 4. In fact, the EDX scans of the PEDOT:PSS deposited on the pPVDF and mPVDF of this GD show very similar mixing depth profiles

DOI: 10.1021/acsami.5b04578
ACS Appl. Mater. Interfaces 2015, 7, 19966−19977

Scheme 3. Illustration of Interactions between PEDOT:PSS Doped with PEG400, PVDF and PVDF-*graft*-PEGMA and the Most Likely Interface Failure Place[a]

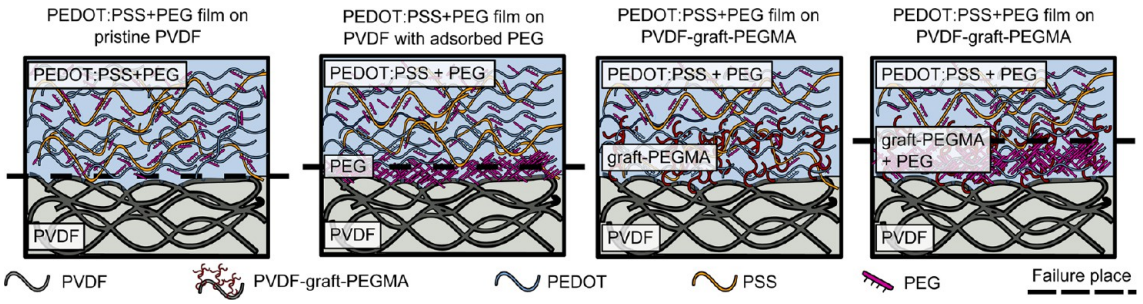

[a]Dashed line indicates the most likely location of interface failure.

(see Figures S7a and S7b in the Supporting Information). Nevertheless, as PEDOT:PSS wets the mPVDF surface (Figures S8 in the Supporting Information) and infiltrates into the pores, the contact area should become significantly larger. Moreover, if infiltrated, there is a PEDOT:PSS film that is formed in the pores and outside during the evaporation of the solvent. That will cause a direct mechanical interlocking. Two experiments were used to test the importance of mechanical interlocking on the adhesion.

Sufficiently low surface tension (γ_L) of a casted solution causes the wetting of the membrane and penetration of it through the pores.[50] The critical γ_L value for pPVDF (pore size of 100 nm, porosity = 70%) was estimated via the "penetrating drop method" and is ~35 mN/m.[50] In order to decrease the surface tension (γ_L) of the PEDOT:PSS aqueous solution, surfactant (Triton X-100) was used. A quantity of 1 vol % of Triton-X100 reduced the value of γ_L to 18.8 mN/m and caused penetration through pPVDF, as shown in Figure S9a in the Supporting Information. The adhesion at the area where PEDOT:PSS film formed in the pores was sufficiently strong to pass the adhesion test in the dry state and after immersion in the ionic liquid. As pristine PVDF membranes are used, the possibility of the hydrogen bonding and the polymer entanglement is negligible. Therefore, strong adhesion is a clear indication of the effect of mechanical interlocking (a more-detailed discussion is provided in the Supporting Information).

Adhesion was also tested on the flat PVDF film (fPVDF), which was produced by melting the porous PVDF membrane on the silicon wafer above 170° and cooling it. It was then functionalized, leading to a GD value of 0.04 ± 0.01 ng/mm^2 (adhesion test and experimental method provided in the Supporting Information). In this case, only hydrogen bonding and entanglement of the graft-PEGMA and PEDOT:PSS are expected to influence adhesion. In comparison to fPVDF, grafting improved adhesion to PEDOT:PSS (Figure S10 in the Supporting Information). Nevertheless, adhesion was observably weaker, compared to mPVDF membranes, and after Test I, some squares of a grid were removed. Lower adhesion could be a consequence of the smaller contact area in the case of a flat film or lack of interlocking.[23] In any case, interlocking in pores could be used to improve the interface strength.

Because of its mechanical properties (brittleness) and its low conductivity, pristine PEDOT:PSS films are rarely used.[51] Hence, various secondary doping strategies and post-treatments are necessary to enhance its properties.[22,51−55] It is important to investigate the effect of the secondary dopants on the adhesion to the PVDF membrane. In all our experiments mentioned so far, 1 vol % of polyethylene glycol (PEG400) was used as a secondary dopant (films made out of the pristine PEDOT:PSS are brittle and difficult to handle).[51,53] Unexpectedly, poor adhesion was observed when the amount of the PEG400 was increased, as shown in Figures S12 and S13 in the Supporting Information).

PEDOT:PSS film was easily removed from both, pPVDF and mPVDF, when 2 vol % or 5 vol % of PEG400 was added to a PEDOT:PSS aqueous solution before solvent casting. Furthermore, in both cases, PEDOT:PSS penetrated through the membrane, as shown in EDX scans in Figures S12 and S13. This is unexpected, since PEG400 does not decrease the surface tension below the critical low surface tension (the γ_L values of PEDOT:PSS with 2 vol % and 5 vol % PEG400 is 60.3 mN/m and 59.3 mN/m, respectively) and the contact angle with pPVDF remains large (129.3° ± 2.7° and 111.6° ± 1.5° for 5 vol % PEG400 in PEDOT:PSS) on the rough and smooth sides, respectively (Figure S11 in the Supporting Information).

PEG readily adsorbs on the pore walls of PVDF from aqueous solutions and is often used for surface modification.[19,21,34] In a solution of PEDOT:PSS, PEG400 forms hydrogen bonds with both PEDOT and PSS. Hence, the core−shell structure of PEDOT:PSS is disrupted, leading to more entangled and conducting thin films.[53] Nevertheless, as reported by Mengistie et al., more than 1 vol % of PEG400 does not further increase its conductivity.[53] Moreover, we think that an excess of PEG400 remains unbound in solution and preferentially adsorbs on the PVDF or PVDF-*graft*-PEGMA membrane. Hence, a PEG400 layer is created that prevents direct PEDOT:PSS interaction with PVDF or PVDF-*graft*-PEGMA. Since physisorption is not a strong interaction and such coatings are often easily removed, the presence of such a layer could neutralize functionalization effects on adhesion, as shown in Scheme 3.[19,21]

Preferential physisorbtion of PEG400 over PEDOT:PSS could also explain the penetration of PEDOT:PSS through the hydrophobic PVDF membrane. As PEG400 covers PVDF pore walls, their hydrophobicity decreases (Figure S11) and, subsequently, the diffusion of hydrophilic PEDOT and PSS can follow. Pictures of the pPVDF and mPVDF membranes after the removal of PEDOT:PSS, as well as step profiles of PEDOT:PSS distribution along the cross section (with 2−5 vol % of PEG400) shown in Figures S12 and S13) support this observation (further discussion is provided in the Supporting Information).

A summary of these results is represented in Scheme 3. We showed that PVDF and PEDOT:PSS can be joined by direct mechanical interlocking, if a large mixing area is provided.

DOI: 10.1021/acsami.5b04578
ACS Appl. Mater. Interfaces 2015, 7, 19966−19977

Table 1. Geometry and Electrical Properties of Actuators

	grafting density, GD (ng/μm)	thickness of dry membrane, h_{dry} (μm)	PEDOT:PSS electrode thickness, h_{el} (μm)	thickness of interfacial layer, h_{int} (μm)	weight of dry actuator, w_{act} (mg)	weight of absorbed emimTFSI, w_{IL} (mg)	electrode resistance, R_{el} (kΩ)
A1	0.15	123 ± 3.7	20/19	19/27	3.75 ± 0.21	1.9 ± 0.2	4.9/2.4 ± 0.6
A2	0.11	117 ± 5.5	23/19	28/30	3.75 ± 0.22	2.0 ± 0.1	3.7/2.2 ± 0.3
A3	0.05	129 ± 3.7	25/20	5–20	3.75 ± 0.15	2.1 ± 0.2	2.5/1.2 ± 0.3
AP		129 ± 17	36/43		6.89 ± 1.4	2.25 ± 0.1	0.9/0.8 ± 0.08

PEGMA grafted on PVDF allows the infiltration of PEDOT:PSS in the pores of the membrane providing such an area. Furthermore, in this case, only a few micrometers of mixing depth are needed for strong adhesion. Hydrogen bonding or entanglement of polymers when PEDOT:PSS is solvent-casted on the grafted PVDF also play a role in improving adhesion. Finally, we showed that a clean interface between polymers must be ensured. Weak physisorption of molecules such as PEG400 between the PVDF and PEDOT:PSS prevents interaction and entanglement of the polymers, leading to a fast separation of layers. Under these conditions, neither infiltration through the membrane nor PVDF-*graft*-PEGMA aid the adhesion.

2.4. PEDOT:PSS/PVDF-*graft*-PEG/PEDOT:PSS Actuators. Having hybrid PVDF membranes is relevant only if other layers of materials must be attached to the surface while the membrane bulk is kept hydrophobic. This is the case for soft actuators, which are made by depositing two conducting polymer electrodes on the surfaces of the membrane. Partial connection of those electrodes would have adverse effects on their performance and would cause a large power dissipation.[13] In order to demonstrate the benefits of the hybrid membranes with different graft densities, several actuators were produced by drop-casting.[56] Rectangular actuators made of the sandwiched trilayer can produce a bidirectional bending motion once a voltage is applied at one end of the actuator (as shown later in this work in Figure 9). For the characterization of the actuation, the bending motion was recorded and the position of the other end of the actuator was tracked in order to calculate the produced strain. A summary of the geometries and electrical properties of the actuators that were used is shown in Table 1.

For lifetime measurements, as shown in Figure 6a, actuators with a dense grafting density and large interfacial layer (A1), and low grafting density and small interfacial layer (A3), and an actuator produced on pPVDF (AP) are compared. In order to fabricate functional actuators on pPVDF, a 5 vol % PEG400 in PEDOT:PSS was used, causing penetration of PEDOT:PSS through the membrane and resulting in a significantly higher current between electrodes. The resistance between electrodes of AP is 6 orders of magnitude lower than for A1 and A3 (0.36 Ω vs 0.16 MΩ), leading to a large power dissipation during actuation. Nevertheless, it allowed sufficient adhesion between layers to sustain an adsorption of 2.2 mg of emimTFSI ionic liquid.

Slight differences were noticed in ionic liquid adsorption capacity of the different actuators. One hour in ionic liquid is sufficient to saturate the membranes, but actuators with a larger interfacial layer absorb slightly less than less-functionalized membranes (1.9 ± 0.2 mg and 2.1 ± 0.2 mg, respectively). Because of its dense structure, PEDOT:PSS does not absorb ionic liquid and, therefore, the interfacial layer slightly decreases the volume of the membrane that is available for storing liquid. Furthermore, PEDOT:PSS in the interfacial layer probably does not form a good path for electrical conductivity, since the

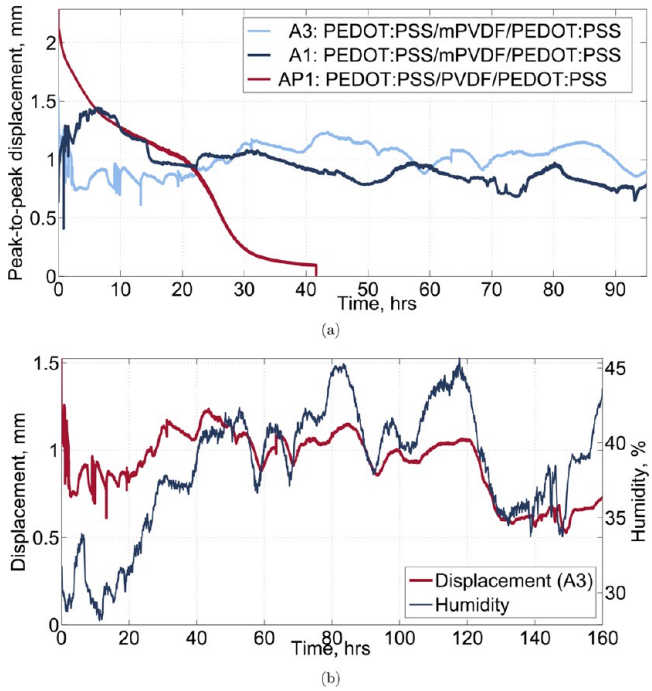

Figure 6. (a) Lifetime measurement of actuators produced with hybrid PVDF-*graft*-PEGMA and pristine membranes. (b) Influence of humidity on the amplitude of the displacement for PEDOT:PSS/PVDF-*graft*-PEG/PEDOT:PSS-based actuator in ionic liquid.

resistance of the electrodes is not only higher for A1 (large interface) in comparison to A3 (small interface) (2.4 ± 0.6 kΩ and 1.2 ± 0.3 kΩ, respectively), but is also different for the two sides of the actuator (4.9 kΩ and 2.4 kΩ, respectively). The same rules do not apply to the AP actuator, because both electrodes are connected and decrease in their density, which leads to thicker electrodes and an easier absorption of ionic liquids.

Nevertheless, once a voltage is applied (at 1.5 V sine wave, 0.1 Hz frequency), the AP actuator displacement amplitude is continuously decreasing and the actuator stops responding after <50 h of actuation. Meanwhile, actuators with even a very small interfacial layer (5 μm) and stronger adhesion remain active for more than 100 h with no significant decrease in displacement amplitude and no signs of delamination. Small variations of amplitude can still be observed and can be explained, as PEDOT:PSS and ionic liquids are hygroscopic materials and can absorb water from the environment. Displacement and humidity of the environment during actuation of the A3 actuator are shown in Figure 6b. Humidity can influence actuation by passive (i.e., Joule) heating-induced reversible absorption and desorption and by changing the PEDOT:PSS microstructure and, consequently, its mechanical and electrical properties.[57,58] Moreover, ionic liquids are also hygroscopic and actuation was shown to be dependent on humidity, even in

DOI: 10.1021/acsami.5b04578
ACS Appl. Mater. Interfaces 2015, 7, 19966–19977

actuators that do not use PEDOT:PSS-based electrodes.[59] In agreement with results published by Must et al., at relatively low frequency and in this humidity range, the actuation amplitude is larger when the humidity is higher.[59] Even though this behavior is reversible and does not cause permanent damage to actuators, humidity should be monitored if the position of the actuator must be controlled. Alternatively, encapsulation of the actuators could be used as a barrier to humidity, but at a cost of the reduced strain and output force.[60,61]

The length of the interfacial layer could influence the performance of actuators, since it influences the thickness of the insulating layer and the electrodes, the electronic conductivity of electrodes, and the amount of the ionic liquid stored in the membrane. Furthermore, the surface area of the electrode, which influences the oxidation and reduction processes, is also dependent on the interfacial layer. Nevertheless, different actuators do not show significant differences, neither in produced strain (Figure 7a) nor in the transferred charge

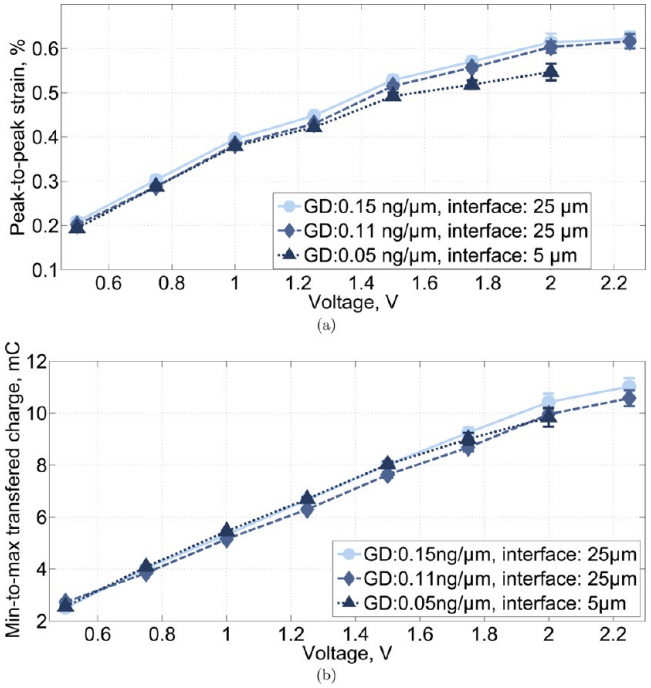

Figure 7. (a) Peak-to-peak strain and (b) transferred charge for actuators with different interfacial layer thickness at various applied voltages.

(Figure 7b) during actuation. Slightly smaller strain is observed for actuators with low interfacial layer at voltages higher than 1.5 V, indicating lower maximum strain during actuation. This can be explained by a slightly greater thickness of the electrodes (25/20 μm for A3 vs 22/19 μm for A1 and A2).[62] A more comprehensive evaluation of the influence of the interfacial layer on actuation and charging rate, blocking force, and maximum strain, as well as ionic conductivity and emimTFSI absorption, etc., is the subject of a future study.

3. CONCLUSIONS

In summary, we demonstrated a technique for the fabrication of hybrid hydrophilic−hydrophobic−hydrophilic PVDF membranes using argon-plasma-induced surface functionalization with PEGMA. We showed that even a small grafting density induces a significant decrease of water contact angle (WCA) from 130° to 20°, leading to a better wetting and adhesion between PEDOT:PSS and PVDF. Furthermore, the deposition depth of the reaction precursor can be tuned if a spray coating is used as a deposition technique. Hybrid PVDF membranes of various thicknesses (ranging from 5 μm to 40 μm) of hydrophobic and hydrophilic layers were obtained. We also studied the factors influencing adhesion between PEDOT:PSS and PVDF membranes and showed that (1) a clean interface with no coating is compulsory for strong binding; (2) membranes pores can lead to a large area of direct mechanical interlocking that also provides strong adhesion; (3) the surface functionalization of the PVDF membrane with hydrophilic PEGMA polymers leads to a stronger adhesion, even with no direct mechanical interlocking. We also showed that utilizing hybrid PVDF-*graft*-PEGMA membranes allows the fabrication of PEDOT:PSS-based actuators that can be operated in air for more than 150 h and 50 000 cycles, and actuation is robust against humidity in the environment. Finally, actuators with different interfacial layers were fabricated and compared. We showed minor influence of the interfacial layer on strain and charging of the actuators.

4. EXPERIMENTAL SECTION

4.1. Materials. Membrane filters that were hydrophobic, with a pore diameter of 0.1 μm, thickness of 125 μm, and diameter of 47 mm) were purchased from Merck Millipore Corp. (Durapore VVHP04700). PEDOT:PSS 1.3 wt % conductivity-grade dispersion in water (No. 483095, Aldrich), having a PEDOT:PSS ratio of 1:2.5 was purchased from Sigma−Aldrich. Polyethylene glycol with a number-average molecular weight of M_n = 400 (PEG400) (No. 202398, Aldrich) was used as a secondary dopant for PEDOT:PSS in order to increase its electrical conductivity[53] and mechanical flexibility. A characterization of the mechanical properties was not conducted in this study, but the effect of PEG is expected to be similar to that of poly(vinyl alcohol) (PVA)[63] and poly(ethylene oxide) (PEO).[16] A quantity of 1 vol % of PEG400 in PEDOT:PSS solution was prepared and maintained at 4 °C before use. Poly(ethylene glycol) monomethyl ether methacrylate (PEGMA) (average M_n = 526) were also purchased from Sigma−Aldrich. A quantity of 10 vol % PEGMA solution in a 10 vol % ethanol and water mixture was prepared and maintained at room temperature before use. Ethyl-methyl-imidazolium bis-(trifluoromethanesulfonyl)imide (emimTFSI) ionic liquid was purchased from Solvionics (No. Im0208a). Other chemicals, such as Triton X-100 and *iso*-butanol, were also obtained from Sigma−Aldrich.

4.2. Functionalization of PVDF Membrane. A schematic illustration of the functionalization of the membranes is shown in Scheme 3. Spray coating (using a Mecafer Ag4 airbrush) was done under the fume hood and inside the glovebox (Captair Pyramid Glovebox) in order to prevent influence of air flow on spray direction. The membrane and the gun were fixed in one line and the gun was slightly moved during the spray while keeping the distance constant. After optimization experiments (Figure S4 in the Supporting Information), the valve opening controlling the droplet size was fixed at half a turn and a pressure of 2 kg_f/cm^3 pressure was used. In order to achieve different grafting densities, the distance of the spray gun to the membrane changed from 25 cm to 35 cm or different amounts (0.5−2.0 mL) were sprayed at 30 cm. For functionalization on both sides, membranes were maintained in air for several minutes between sprays. PVDF membranes were then dried in an oven at 70 °C for 1 h and weighted for spray density calculations (SD represents the amount of PEGMA deposited per area, where the surface area of the PVDF membrane was calculated ignoring porosity and roughness).

Membranes coated with a dried PEGMA monomer layer were then treated by low-pressure plasma with an argon flow rate of 5 sccm, an input power of 10 W, and a bias of 1 W (measured power of 5 W and a bias of 0.2 W), controlled by a 13.56 MHz RF generator (Aviza

DOI: 10.1021/acsami.5b04578
ACS Appl. Mater. Interfaces 2015, 7, 19966−19977

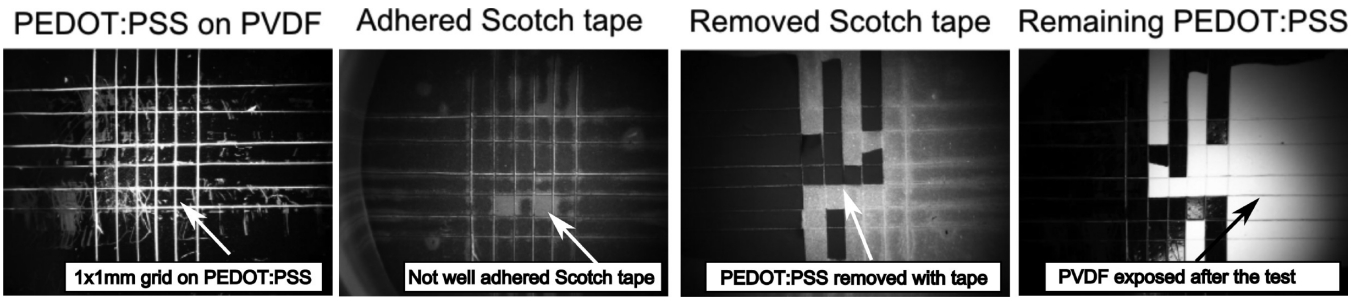

Figure 8. Steps of adhesion evaluation process (from left to right): grid of 25 squares cut on the PEDOT:PSS surface until PVDF membrane; adhesive tape applied on the grid and indication of good adhesion; picture of the adhesive tape after it was removed from the film; and picture of the PVDF membrane and remaining PEDOT:PSS film after the adhesive tape was removed.

Technology, Inc., Model OMEGA201). The low-pressure plasma treatment was operated at a pressure of 50 mTorr. After plasma treatment, the PEGylated PVDF membrane was maintained in air for at least 72 h to neutralize radicals on the PVDF backbone.[64] The nonreacted PEGMA monomer was removed by washing membranes in an ultrasonic bath in water, ethanol, and again in water for 1 h each. The remaining solvent was removed by drying membranes in the oven of 70 °C for 2 h. The membranes were weighted again for grafting density calculations (weight difference after and before treatment per surface area, without taking into account grafting depth and roughness).

4.3. Characterization of PVDF Membrane. Fourier transform infrared (FTIR) spectrophotometry in ATR mode with GaSn crystal as a reflection element (Bruker Optics, Model VERTEX 70) was done for surface chemical characterization. Sixty four (64) scans at a resolution of 4 cm^{-1} were averaged. The obtained spectrum were further used for numerical integration of peaks, corresponding to OCO and CF bond vibrations from 1700 cm^{-1} to 1750 cm^{-1} and from 1390 cm^{-1} to 1420 cm^{-1}, respectively (indicated in Figure 2a). The ratio of integrated peaks was used to characterize surface coverage by PVDF-*graft*-PEGMA of the membranes. DI water contact angle measurements, as well as PEDOT:PSS solutions contact angle measurements, were performed at a temperature of 25 °C with a Digidrop GBX Contact Angle Meter (the results of five different measurements were averaged). Digidrop GBX was also used for the surface tension measurements of various PEDOT:PSS, using the pendent drop method. Atomic force microscopy (AFM) of functionalized and pristine membranes was performed with Veeco-Dimension Icon AFM (Veeco) in tapping mode, using RTESP-300 AFM probes (resonance frequency of ∼300 kHz), and the averaged roughness was calculated using the NanoScope Analysis software (Veeco).

For estimation of the grafting depth, modified PVDF membranes were fixed in a ⌀45 mm aluminum clamp and 3 mL of PEDOT:PSS solution (with 1 vol % PEG400) were solvent-casted. They then were dried for 24 h in air and 2 h at 70 °C. Membranes were fractured in liquid N_2 in order to obtain clean cross-sections. The distribution of sulfur (the signature element of PEDOT:PSS) and fluorine (the signature element of PVDF) were mapped by an energy-dispersive X-ray (EDX) spectrometer (Helios NanoLab 600i, accelerating voltage = 5 kV, working distance = 6 mm) in linear scan and map scan modes. The length of the overlap of both signals was determined.

4.4. Adhesion Evaluation. To characterize the adhesion, a qualitative cross-cut adhesive tape peeling test (similar to ISO 2409:2013 recommendations) was performed (Figure 8). Three milliliters (3 mL) of the PEDOT:PSS aqueous solution with various secondary dopants and surfactants were deposited on PVDF membranes by solvent casting, dried overnight, and for 2 h at 80 °C (equivalent to preparation of actuators). The PEDOT:PSS film (10−50 μm, depending on infiltration width and density of the film) was formed. Two series of parallel cuts then were cross-angled to each other to obtain a pattern of 25 similar squares was cut using surgical scalpel through the PEDOT:PSS film but not slitting the PVDF membrane. The membrane with the cut grid was attached to solid support, adhesive tape (Scotch Magic tape) was pressed down by hand until the tape was homogeneously adhered (color indicator) and was slowly pulled off at a 90° angle. The PEDOT:PSS remaining on the adhesive tape, as well as on the PVDF membrane, was evaluated. The method was previously used and validated by Liu et al.[6]

4.5. Fabrication of Actuators. For the fabrication of actuators with different mixing depths, functionalized membranes were fabricated by spraying 0.5, 1.0, and 2.0 mL of PEGMA resulting in GD values of 0.15, 0.10, and 0.03 ng/mm^2. After drying, they were fixed in a ⌀45 mm aluminum clamp and 3 mL of PEDOT:PSS, secondary doped with 1 vol % of PEG400, were drop-casted. Membranes were then dried in air in UV-reduced environment for at least 20 h. The other side of the membrane was processed in the same way. The membranes then were thermally annealed in oven for 2 h at 70 °C. Strips with dimensions of 2 mm × 1.5 cm were cut, using a CO_2 laser (power = 45 W, speed = 100 cm/s, 1000 Hz; Trotec FineMarker Hybrid). Each actuator was then weighted and its thickness measured. They were kept in emimTFSI for 1.5 h before lifetime measurement experiments or 24 h for strain characterization. After soaking, their weight and thickness were measured again.

4.6. Characterization of Actuators. The thickness of dry and soaked actuators was measured using a digimatic indicator (Mitutoyo Absolute) and also estimated from the scanning electron microscopy (SEM) photomicrographs. SEM images of membranes and actuators were obtained using a Hitachi Model S-4800 field-emission scanning electron microscope (acceleration voltage = 800 V, working distance ≈ 5 mm). Electronic conductivity of PEDOT:PSS was measured between two extremes of each electrode and between two electrodes, by applying a voltages up to 0.1−0.5 V and measuring the current, using a Suss Model PA200 probe station and an Agilent Model 4142B tester.

For all mechanical characterization measurements, actuators were placed between two copper electrodes clamped at 1−2 mm from one end of the actuator, as shown in Figure 9. For maximum bending measurements, actuators were placed under a microscope (Leica Microsystems, Model MZ-12) with a Digital Sight camera system (Nikon). The square voltage wave with various amplitudes and frequencies was generated with a Keithley Model 2450 sourcemeter. Bending was recorded at a rate of 5 frames per second (640 × 480 resolution). Videos there further processed using the Matlab Image processing toolbox to track the displacement of the actuator tip (shown as a green line in Figure 9) . The strain was then calculated from tip displacement using formulas proposed by Sugino et al.:[65]

$$\epsilon\,(\%) = \frac{2hd}{L^2 + d^2} \times 100 \qquad (1)$$

where ϵ is the strain (expressed as a percentage); h, L, and d are the thickness, free length, and displacement of the actuator, respectively. The thickness of a dry actuator, estimated by SEM, was used for the calculations.

Lifetime measurements were recorded by laser displacement sensor (Model optoNCDT 1302, MicroEpsilon) at the position of ∼2 mm from the end of the actuator at actuation with a 1.5 V sine wave of 0.1 Hz.

DOI: 10.1021/acsami.5b04578
ACS Appl. Mater. Interfaces 2015, 7, 19966−19977

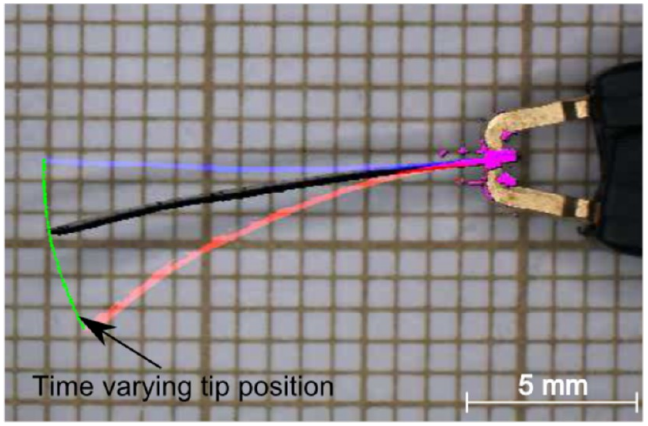

Figure 9. Merged images of the A3 actuator at the initial position and its extremes during actuation, obtained by applying a square wave with a frequency of 50 mHz and an amplitude of 2.25 V. Blue and red actuators show its maximum and minimum displacement position, respectively; green dots show the tip position calculated from recorded videos. Actuator is bending toward the negative electrode.

■ ASSOCIATED CONTENT

Supporting Information

The Supporting Information is available free of charge on the ACS Publications website at DOI: 10.1021/acsami.5b04578.

Results of the preliminary experiments testing different precursor deposition techniques (Figures S1–S3); spraying efficiency under different conditions (Figure S4); AFM images and FTIR graphs showing results of the experiments with various grafting times (Figure S5); AFM images of surfaces after grafting different amounts of PEG (Figure S6); contact angle measurements, EDX scans along the cross-section (Figure S7) and adhesion measurements of PVDF and PEDOT:PSS on flat films (Figure S8), with PEDOT:PSS and surfactants (Figures S9 and S10) and with different secondary dopants (Figures S11–S14) (PDF)

Video (AVI)

■ AUTHOR INFORMATION

Corresponding Authors

*E-mail: asimaite@laas.fr (A. Simaite).

*E-mail: bergaud@laas.fr (C. Bergaud).

Notes

The authors declare no competing financial interest.

■ ACKNOWLEDGMENTS

The authors acknowledge the French Ministry of Defence, The Armaments Procurement Agency (DGA) for the Ph.D. grant for work on Development of electroactive polymer-based actuators for actuation in robotics. This work was partly supported by the French RENATECH Network.

■ REFERENCES

(1) Mirfakhrai, T.; Madden, J. D. W.; Baughman, R. H. Polymer Artificial Muscles. *Mater. Today (Oxford, U. K.)* **2007**, *10*, 30–38.

(2) Madden, P. G.; Madden, J. D.; Anquetil, P.; Vandesteeg, N.; Hunter, I. W. The Relation of Conducting Polymer Actuator Material Properties to Performance. *IEEE J. Oceanic Eng.* **2004**, *29*, 696–705.

(3) Smela, E. Conjugated Polymer Actuators for Biomedical Applications. *Adv. Mater. (Weinheim, Ger.)* **2003**, *15*, 481–494.

(4) Punning, A.; Must, I.; Põldsalu, I.; Vunder, V.; Temmer, R.; Kruusamäe, K.; Kaasik, F.; Torop, J.; Rinne, P.; Lulla, T.; Johanson, U.; Tamm, T.; Aabloo, A. Lifetime Measurements of Ionic Electroactive Polymer Actuators. *J. Intell. Mater. Syst. Struct.* **2014**, *25*, 2267–2275.

(5) *Electroactive Polymer (EAP) Actuators as Artificial Muscles: Reality, Potential, and Challenges*; Chapter 7; Bar-Cohen, Y., Ed.; SPIE Press: Bellingham, WA, USA, 2004; ISBN: 0819452971 (0-8194-5297-1).

(6) Liu, Y.; Gan, Q.; Baig, S.; Smela, E. Improving PPy Adhesion by Surface Roughening. *J. Phys. Chem. C* **2007**, *111*, 11329–11338.

(7) Bennett, M. D.; Leo, D. J. Ionic Liquids as Stable Solvents for Ionic Polymer Transducers. *Sens. Actuators, A* **2004**, *115*, 79–90.

(8) Lu, W.; Fadeev, A. G.; Qi, B.; Smela, E.; Mattes, B. R.; Ding, J.; et al. Use of Ionic Liquids for π-conjugated Polymer Electrochemical Devices. *Science* **2002**, *297*, 983–987.

(9) Vidal, F.; Plesse, C.; Teyssié, D.; Chevrot, C. Long-life Air Working Conducting Semi-IPN/ionic Liquid Based Actuator. *Synth. Met.* **2004**, *142*, 287–291.

(10) Okuzaki, H.; Takagi, S.; Hishiki, F.; Tanigawa, R. Ionic Liquid/polyurethane/PEDOT:PSS Composites for Electro-active Polymer Actuators. *Sens. Actuators, B* **2014**, *194*, 59–63.

(11) Temmer, R.; Must, I.; Kaasik, F.; Aabloo, A.; Tamm, T. Combined Chemical and Electrochemical Synthesis Methods for Metal-Free Polypyrrole Actuators. *Sens. Actuators, B* **2012**, *166-167*, 411–418.

(12) Temmer, R.; Maziz, A.; Plesse, C.; Aabloo, A.; Vidal, F.; Tamm, T. In Search of Better Electroactive Polymer Actuator Materials: PPy versus PEDOT versus PEDOT-PPy Composites. *Smart Mater. Struct.* **2013**, *22*, 104006.

(13) Festin, N.; Plesse, C.; Pirim, P.; Chevrot, C.; Vidal, F. Electro-Active Interpenetrating Polymer Networks Actuators and Strain Sensors: Fabrication, Position Control and Sensing Properties. *Sens. Actuators, B* **2014**, *193*, 82–88.

(14) Li, Y.; Tanigawa, R.; Okuzaki, H. Soft and Flexible PEDOT/PSS Films for Applications to Soft Actuators. *Smart Mater. Struct.* **2014**, *23*, 074010.

(15) Kim, S.-S.; Jeon, J.-H.; Kee, C.-D.; Oh, I.-K. Electro-active Hybrid Actuators Based on Freeze-dried Bacterial Cellulose and PEDOT:PSS. *Smart Mater. Struct.* **2013**, *22*, 085026.

(16) Ikushima, K.; John, S.; Ono, A.; Nagamitsu, S. PEDOT/PSS Bending Actuators for Autofocus Micro Lens Applications. *Synth. Met.* **2010**, *160*, 1877–1883.

(17) Dupont, S. R.; Oliver, M.; Krebs, F. C.; Dauskardt, R. H. Interlayer Adhesion in Roll-to-roll Processed Flexible Inverted Polymer Solar Cells. *Sol. Energy Mater. Sol. Cells* **2012**, *97*, 171–175.

(18) Angelo, P. D.; Farnood, R. R. Poly(3,4-Ethylenedioxythiophene): Poly (Styrene Sulfonate) Inkjet Inks Doped with Carbon Nanotubes and a Polar Solvent: The Effect of Formulation and Adhesion on Conductivity. *J. Adhes. Sci. Technol.* **2010**, *24*, 643–659.

(19) Kang, G.-d.; Cao, Y.-m. Application and Modification of Poly(vinylidene fluoride) (PVDF) Membranes—A Review. *J. Membr. Sci.* **2014**, *463*, 145–165.

(20) Dalvi, V. H.; Rossky, P. J. Molecular Origins of Fluorocarbon Hydrophobicity. *Proc. Natl. Acad. Sci. U. S. A.* **2010**, *107*, 13603–13607.

(21) Liu, F.; Hashim, N. A.; Liu, Y.; Abed, M. M.; Li, K. Progress in the Production and Modification of PVDF Membranes. *J. Membr. Sci.* **2011**, *375*, 1–27.

(22) Xia, Y.; Sun, K.; Ouyang, J. Solution-Processed Metallic Conducting Polymer Films as Transparent Electrode of Optoelectronic Devices. *Adv. Mater. (Weinheim, Ger.)* **2012**, *24*, 2436–2440.

(23) Awaja, F.; Gilbert, M.; Kelly, G.; Fox, B.; Pigram, P. J. Adhesion of Polymers. *Prog. Polym. Sci.* **2009**, *34*, 948–968.

(24) Jin, X.; Heepe, L.; Strueben, J.; Adelung, R.; Gorb, S. N.; Staubitz, A. Challenges and Solutions for Joining Polymer Materials. *Macromol. Rapid Commun.* **2014**, *35*, 1551–1570.

(25) Cui, L.; Ranade, A. N.; Matos, M. A.; Dubois, G.; Dauskardt, R. H. Improved Adhesion of Dense Silica Coatings on Polymers by Atmospheric Plasma Pretreatment. *ACS Appl. Mater. Interfaces* **2013**, *5*, 8495–8504.

DOI: 10.1021/acsami.5b04578
ACS Appl. Mater. Interfaces 2015, 7, 19966–19977

(26) Petersen, J.; Fouquet, T.; Michel, M.; Toniazzo, V.; Dinia, A.; Ruch, D.; Bomfim, J. A. S. Enhanced Adhesion over Aluminum Solid Substrates by Controlled Atmospheric Plasma Deposition of Amine-rich Primers. *ACS Appl. Mater. Interfaces* **2012**, *4*, 1072−1079.
(27) Maeda, N.; Chen, N.; Tirrell, M.; Israelachvili, J. N. Adhesion and Friction Mechanisms of Polymer-on-Polymer Surfaces. *Science* **2002**, *297*, 379−382.
(28) Morita, H.; Yamada, M.; Yamaguchi, T.; Doi, M. Molecular Dynamics Study of the Adhesion between End-grafted Polymer Films. *Polym. J. (Tokyo, Jpn.)* **2005**, *37*, 782−788.
(29) Chen, K.-S.; Uyama, Y.; Ikada, Y. Adhesive Interaction between Polymer Surfaces Grafted with Water-soluble Polymer Chains. *Langmuir* **1994**, *10*, 1319−1322.
(30) Takahashi, J.; Hotta, A. Adhesion Enhancement of Polyolefins by Diamond Like Carbon Coating and Photografting Polymerization. *Diamond Relat. Mater.* **2012**, *26*, 55−59.
(31) Chang, Y.; Ko, C.-Y.; Shih, Y.-J.; Quémener, D.; Deratani, A.; Wei, T.-C.; Wang, D.-M.; Lai, J.-Y. Surface Grafting Control of PEGylated Poly(vinylidene fluoride) Antifouling Membrane via Surface-initiated Radical Graft Copolymerization. *J. Membr. Sci.* **2009**, *345*, 160−169.
(32) Wang, J. J.; Liu, F. Imparting Antifouling Properties of Silicone Hydrogels by Grafting Poly(ethylene glycol) Methyl Ether Acrylate Initiated by UV Light. *J. Appl. Polym. Sci.* **2012**, *125*, 548−554.
(33) Chang, Y.; Shih, Y.-j.; Ko, C.-y.; Jhong, J.-f.; Liu, Y.-l.; Wei, T.-c. Hemocompatibility of Poly(vinylidene fluoride) Membrane Grafted with Network-Like and Brush-Like Antifouling Layer Controlled via Pegylation, Plasma-induced Surface. *Langmuir* **2011**, *27*, 5445−5455.
(34) Wang, P.; Tan, K.; Kang, E.; Neoh, K. Plasma-induced Immobilization of Poly(ethylene glycol) onto Poly(vinylidene fluoride) Microporous Membrane. *J. Membr. Sci.* **2002**, *195*, 103−114.
(35) Zhao, Z.-P.; Li, M.-S.; Li, N.; Wang, M.-X.; Zhang, Y. Controllable Modification of Polymer Membranes by Long-distance and Dynamic Low-temperature Plasma Flow: AA Grafting Penetrated through Electrospun PP Fibrous Membranes. *J. Membr. Sci.* **2013**, *440*, 9−19.
(36) Chang, Y.; Shih, Y.-J.; Ruaan, R.-C.; Higuchi, A.; Chen, W.-Y.; Lai, J.-Y. Preparation of Poly(vinylidene fluoride) Microfiltration Membrane with Uniform Surface-copolymerized Poly(ethylene glycol) Methacrylate and Improvement of Blood Compatibility. *J. Membr. Sci.* **2008**, *309*, 165−174.
(37) Kaur, S.; Ma, Z.; Gopal, R.; Singh, G.; Ramakrishna, S.; Matsuura, T. Plasma-induced graft Copolymerization of Poly-(methacrylic acid) on Electrospun Poly(vinylidene fluoride) Nanofiber Membrane. *Langmuir* **2007**, *23*, 13085−13092.
(38) Choi, Y.-j.; Moon, S.-h.; Yamaguchi, T.; Nakao, S.-i. New Morphological Control for Thick, Porous Membranes with a Plasma Graft-Filling Polymerization. *J. Polym. Sci., Part A: Polym. Chem.* **2003**, *41*, 1216−1224.
(39) Bernardelli, E. A.; Mafra, M.; Maliska, A. M.; Belmonte, T.; Klein, A. N. Influence of Neutral and Charged Species on the Plasma Degradation of the Stearic Acid. *Mater. Res.* **2013**, *16*, 385−391.
(40) Sukhishvili, S. A.; Chen, Y.; Müller, J. D.; Gratton, E.; Schweizer, K. S.; Granick, S. Surface Diffusion of Poly(ethylene glycol). *Macromolecules (Washington, DC, U.S.)* **2002**, *35*, 1776−1784.
(41) Linse, P.; Kallrot, N. Polymer Adsorption from Bulk Solution onto Planar Surfaces: Effect of Polymer Flexibility and Surface Attraction in Good Solvent. *Macromolecules (Washington, DC, U.S.)* **2010**, *43*, 2054−2068.
(42) Zhao, J.; Granick, S. How Polymer Surface Diffusion Depends on Surface Coverage. *Macromolecules (Washington, DC, U.S.)* **2007**, *40*, 1243−1247.
(43) Skaug, M. J.; Mabry, J. N.; Schwartz, D. K. Single-Molecule Tracking of Polymer Surface Diffusion. *J. Am. Chem. Soc.* **2014**, *136*, 1327−1332.
(44) Wenzel, R. Resistance of Solid Surfaces. *Ind. Eng. Chem.* **1936**, *28*, 988−994.
(45) Cole, P. J.; Cook, R. F.; Macosko, C. W. Adhesion Between Immiscible Polymers Correlated with Interfacial Entanglements. *Macromolecules (Washington, DC, U.S.)* **2003**, *36*, 2808−2815.
(46) Ge, T.; Grest, G. S.; Robbins, M. O. Tensile Fracture of Welded Polymer Interfaces: Miscibility, Entanglements, and Crazing. *Macromolecules (Washington, DC, U.S.)* **2014**, *47*, 6982−6989.
(47) Kato, K.; Uchida, E.; Kang, E.-T.; Uyama, Y.; Ikada, Y. Polymer Surface with Graft Chains. *Prog. Polym. Sci.* **2003**, *28*, 209−259.
(48) Kim, S.-S.; Jeon, J.-H.; Kee, C.-D.; Oh, I.-K. Electro-Active Hybrid Actuators Based on Freeze-Dried Bacterial Cellulose and PEDOT:PSS. *Smart Mater. Struct.* **2013**, *22*, 085026.
(49) Rezaei Kolahchi, A.; Carreau, P. J.; Ajji, A. Surface Roughening of PET Films through Blend Phase Coarsening. *ACS Appl. Mater. Interfaces* **2014**, *6*, 6415−6424.
(50) Franken, a. C. M.; Nolten, J.; Mulder, M.; Bargeman, D.; Smolders, C. Wetting Criteria for the Applicability of Membrane Distillation. *J. Membr. Sci.* **1987**, *33*, 315−328.
(51) Lang, U.; Naujoks, N.; Dual, J. Mechanical Characterization of PEDOT:PSS Thin Films. *Synth. Met.* **2009**, *159*, 473−479.
(52) Ouyang, J. Secondary Doping Methods to Significantly Enhance the Conductivity of PEDOT:PSS for Its Application as Transparent Electrode of Optoelectronic Devices. *Displays* **2013**, *34*, 423−436.
(53) Alemu Mengistie, D.; Wang, P.-C.; Chu, C.-W. Effect of Molecular Weight of Additives on the Conductivity of PEDOT:PSS and Efficiency for ITO-Free Organic Solar Cells. *J. Mater. Chem. A* **2013**, *1*, 9907−9915.
(54) Döbbelin, M.; Marcilla, R.; Salsamendi, M.; Pozo-Gonzalo, C.; Carrasco, P. M.; Pomposo, J. A.; Mecerreyes, D. Influence of Ionic Liquids on the Electrical Conductivity and Morphology of PEDOT:PSS Films. *Chem. Mater.* **2007**, *19*, 2147−2149.
(55) Huang, J.; Miller, P.; de Mello, J.; de Mello, A. J.; Bradley, D. Influence of Thermal Treatment on the Conductivity and Morphology of PEDOT/PSS Films. *Synth. Met.* **2003**, *139*, 569−572.
(56) Simaite, A.; Tondu, B.; Mathieu, F.; Souéres, P.; Bergaud, C. Simple Casting Based Fabrication of PEDOT:PSS-PVDF-Ionic Liquid Soft Actuators. *Proc. SPIE* **2015**, *9430*, 94301E.
(57) Taccola, S.; Greco, F.; Sinibaldi, E.; Mondini, A.; Mazzolai, B.; Mattoli, V. Toward a New Generation of Electrically Controllable Hygromorphic Soft Actuators. *Adv. Mater. (Weinheim, Ger.)* **2015**, *27*, 1668−1675.
(58) Zhou, J.; Anjum, D. H.; Chen, L.; Xu, X.; Ventura, I. A.; Jiang, L.; Lubineau, G. The Temperature-dependent Microstructure of PEDOT/PSS Films: Insights from Morphological, Mechanical and Electrical Analyses. *J. Mater. Chem. C* **2014**, *2*, 9903−9910.
(59) Must, I.; Vunder, V.; Kaasik, F.; Poldsalu, I.; Johanson, U.; Punning, A.; Aabloo, A. Ionic Liquid-based Actuators Working in Air: The Effect of Ambient Humidity. *Sens. Actuators, B* **2014**, *202*, 114−122.
(60) Madden, J. D.; Cush, R. A.; Kanigan, T. S.; Brenan, C. J.; Hunter, I. W. Encapsulated Polypyrrole Actuators. *Synth. Met.* **1999**, *105*, 61−64.
(61) Naficy, S.; Stoboi, N.; Whitten, P. G.; Spinks, G. M.; Wallace, G. G. Evaluation of Encapsulating Coatings on the Performance of Polypyrrole Actuators. *Smart Mater. Struct.* **2013**, *22*, 075005.
(62) Melling, D.; Wilson, S.; Jager, E. W. H. The Effect of Film Thickness on Polypyrrole Actuation Assessed Using Novel Non-contact Strain Measurements. *Smart Mater. Struct.* **2013**, *22*, 104021.
(63) Romyen, N.; Thongyai, S.; Praserthdam, P.; Sotzing, G. A. Enhancement of Poly(3,4-Ethylenedioxy Thiophene)/Poly(Styrene Sulfonate) Properties by Poly(Vinyl Alcohol) and Doping Agent as Conductive Nano-Thin Film for Electronic Application. *J. Mater. Sci.: Mater. Electron.* **2013**, *24*, 2897−2905.
(64) Park, Y.; Inagaki, N. Surface modification of poly (vinylidene fluoride) film by remote Ar, H_2, and O_2 plasmas. *Polymer* **2003**, *44*, 1569−1575.
(65) Sugino, T.; Kiyohara, K.; Takeuchi, I.; Mukai, K.; Asaka, K. Actuator Properties of the Complexes Composed by Carbon Nanotube and Ionic Liquid: The Effects of Additives. *Sens. Actuators, B* **2009**, *141*, 179−186.

DOI: 10.1021/acsami.5b04578
ACS Appl. Mater. Interfaces 2015, 7, 19966−19977